Title

ABSTRACT

Subject headings: Sun: activity; Sun: corona; Sun: coronal mass ejections (CMEs)

1. Introduction

2. Numerical Differentiation & Error Propagation (recap)

When presented with a moving object through a sequence of image frames such that it is possible to measure its position at each time step, the technique of numerical differentiation is often used to derive the velocity and acceleration of the object. In the standard 2-point approach, it should be possible to derive the time evolution of a system at time step $t + \delta t$ according to the system values at time step t. This may be applied through the technique of forward, reverse or centre differencing, resulting in an estimate of the speed of the object at a specific time step given its positional information. More commonly, a 3-point Lagrangian interpolation is applied to better approximate the kinematics of a moving object by solving for the Lagrange polynomials that best fit across three given datapoints (e.g. DERIV.PRO in IDL). Each of these schemes is based upon the Taylor series expansion of a real function $f(t)$:

$$f(t_0+\delta t) \;=\; f(t_0)+f'(t_0)\delta t+\frac{f''(t_0)}{2!}(\delta t)^2+... \quad (1)$$

but due to the approximation of an infinite series with a finite number of terms and iterations, an error must be associated with the result, based on its deviation from the true solution. Generally the Euler method is employed, using the formula:

$$y_{n+1} \;=\; y_n + hf(t_n, y_n) \quad (2)$$

to solve the initial value problem $y' = f(t, y)$ given $y(t_0) = y_0$, where h is the stepsize such that $t_n = t_0 + nh$. The convergence of such an approximation to the actual solution is prone to two sources of error; truncation error (the difference between the true solution and the approximation) and round-off error (the limited precision of the approximation). Add to this fact that the data measurements themselves are subject to uncertainties in both the positional and temporal information, and the ability of the numerical differentiation techniques to derive kinematics becomes highly jeopardised, as shall be shown.

Given a function $x = f(u, v)$, the error propagation equation (based on the standard deviations σ of the variables) is written:

$$\sigma_x^2 \;=\; \sigma_u^2\left(\frac{\partial x}{\partial u}\right)^2+\sigma_v^2\left(\frac{\partial x}{\partial v}\right)^2+2\sigma_{uv}^2\left(\frac{\partial x}{\partial u}\right)\left(\frac{\partial x}{\partial v}\right)+... \quad (3)$$

Specifically in the case of kinematic analyses, this is used to propagate the errors on the height-time data $r(t)$ into the velocity $v(t)$ and acceleration $a(t)$ profiles to determine the associated uncertainties. In the case of height-time data the covariance terms are zero because the quantities are uncorrelated.

In the case of relatively low sampling of the data, as in the case of coronagraph observations of CMEs, it is generally found that the simplest differentiation techniques are not applicable. The forward and/or reverse differencing techniques act to shift the kinematic profiles by one time-step, which is substantial enough to be of concern here (i.e., they derive a result at the current time-step, based on the pro-/preceeding time-step). Centre differencing employs the two neighbouring datapoints of the point under examination, and so is a better indication of the result at that time-step, but it fails at both endpoints. In any case these should not be employed when the spacing of the datapoints is unequal, i.e., when the cadence δt is not constant, and so the 3-point Lagrangian interpolation technique is used for such cases (and gives the same result as the centre-difference otherwise, but includes the endpoints). The Lagrangian in-

terpolation polynomial is given by:

$$L(x) = \sum_{j=0}^{2} y_j l_j(x) \quad (4)$$

$$\text{where} \quad l_j(x) = \prod_{i=0, i\neq j}^{2} \frac{x-x_i}{x_j-x_i} \quad (5)$$

The derivative at point x is given by $L' = \partial_x L(x)$. So for the case of height-time data being used to derive velocity (and similarly for acceleration) the associated error is given by:

$$\sigma_{v_1}^2 = \frac{\sigma_{r(t_2)}^2 + \sigma_{r(t_0)}^2}{(t_2-t_0)^2} + v^2 \left(\frac{\sigma_{t_2}^2 + \sigma_{t_0}^2}{(t_2-t_0)^2} \right) \quad (6)$$

with the endpoint errors derived from a weighting of the pro-/preceeding two datapoints, that is therefore larger to reflect the uncertainty of the trend beyond the sample points.

Although the 3-point Lagrangian is mathematically sound, its application to CME data has proved problematic due to the limitations of the data. The main drawback is that the noise level across the few, low-cadence measurements, often belies the actual trends of the data such that the numerical derivations of velocity and acceleration become untrustworthy and even misleading. As an example of this, we simulate a height-time profile of a CME that propagates with a constant acceleration of 2 m s^{-2} and initial velocity 300 km s^{-1}, and add random noise of various levels up to a maximum of ∼20%. An errorbar on each datapoint is determined by its distance from the true height-time profile, to represent the worst best-case scenario wherein all measurements lie on the very edge of the known error. Various instances of datapoint scatters result in erroneous trends in the velocity and acceleration profiles - even with the proper error treatment ascribed by the 3-point Lagrangian interpolation technique. Two such cases are shown in Figure 1 where completely opposing acceleration trends are revealed, indicating that the nature of the scatter in the samples is not satisfactorily reflected in the derived kinematics and associated errors. The worry here is that for CMEs undergoing non-constant acceleration, the resulting trends in the derived profiles may be completely intractable via these methods. One possible assurance has been that instead of trusting the endpoints, even given their larger errorbars, they be removed. Figure 1 would then show three datapoints for CME velocity and one for acceleration, that would in the left case go somewhat toward removing the biased trend and implying a constant acceleration, while in the right case it would remain inconclusive. So qualitatively this might achieve a more accurate result and avoid assigning erroneous trends, especially to fast CMEs for which there are few datapoints.

Beyond the interest certainly in the initial acceleration from the forces that drive a CME to erupt, there is a real physical motivation to resolve the subsequent low or zero acceleration as precisely as possible. This is important for determining whether the predominant forces acting are such that the CME is, in general, undergoing continued driving (internal) forces, or positive or negative drag (external) forces, or most assuredly some interplay of both. Any changes to its acceleration that result from different phases of dominating force, and where or why this occurs, are of great interest. Yet this all remains somewhat elusive given the limitations of current CME data, especially as Wen et al. (2007) demonstrate that the errors in the acceleration values can be of the same order as the accelerations typically measured.

We investigate the output of the recently developed CORIMP catalogue with new techniques (and stringent error analyses) for deriving CME kinematics.

3. Techniques

3.1. Testing for non-constant acceleration with the 3-point Lagrangian

We investigate the effect of the cadence of the observations on the derivation of the kinematics and associated errorbars using the standard 3-point Lagrangian interpolation. A theoretical CME with non-constant acceleration is modeled by the following kinematic profile equations (as used in Byrne et al. 2012 based on a variation of the acceleration function chosen by Gallagher et al. 2003):

$$h(t) = \sqrt{2x}\, t \tan^{-1}\left(\frac{e^{t/2x}}{\sqrt{2x}}\right) \quad (7)$$

$$v(t) = \sqrt{2x} \tan^{-1}\left(\frac{e^{t/2x}}{\sqrt{2x}}\right) + \frac{e^{t/2x} t}{e^{t/x}+2x} \quad (8)$$

$$a(t) = \frac{e^{t/2x}\left(2x(t+4x) - e^{t/x}(t-4x)\right)}{2x\left(e^{t/x}+2x\right)^2} \quad (9)$$

where x is just a scaling factor, set to be con-

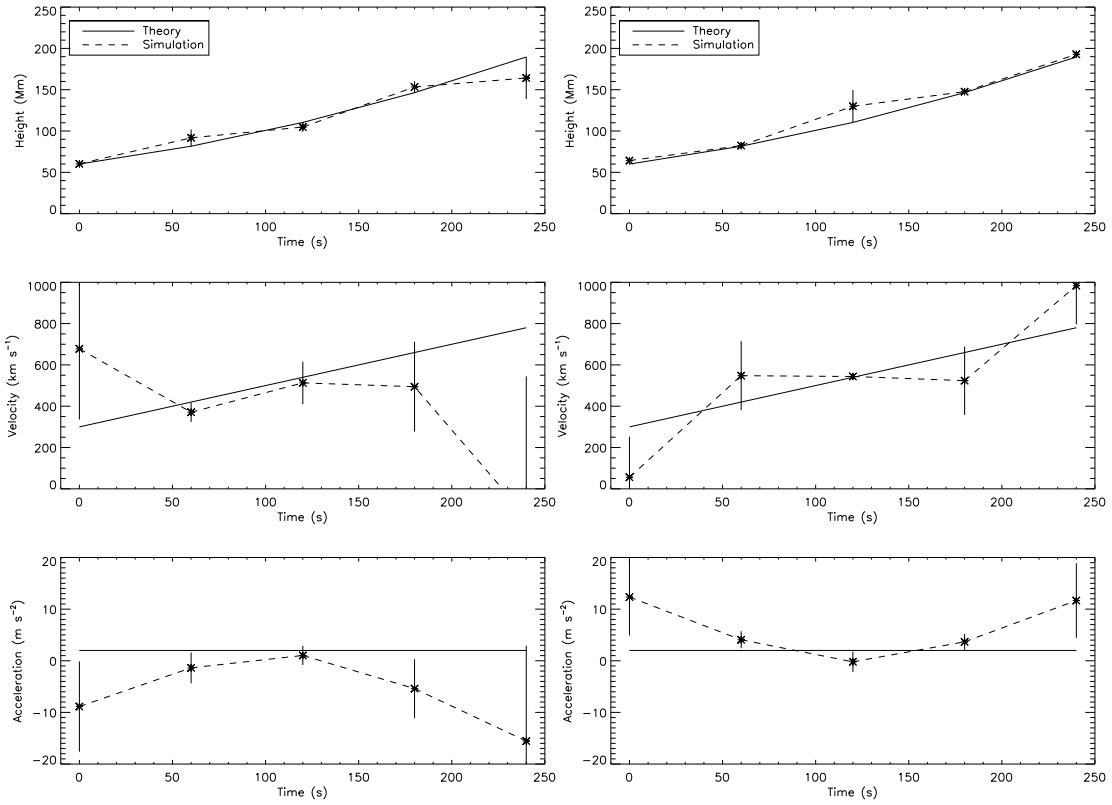

Fig. 1.— A theoretical model for a CME with constant acceleration 2 m s^{-2} and initial velocity 300 km s^{-1}, and two simulations of how the resulting profiles for a noisy sample of datapoints behave using 3-point Lagrangian interpolation.

stant. The resulting acceleration profile exhibits an initial peak followed by a deceleration and then leveling to zero. This is akin to a general impulsive CME that undergoes an initial high-acceleration eruptive phase, and then decelerates to match the solar wind speed during its propagation phase. Thus a model CME height-time profile is generated enabling synthetic observation samples to be taken at different cadences from $1-47$ mins. In the first instance fixed $1\,\sigma$ errorbars of approximately $\pm\,25$ Mm are applied to the height-time points, without any noise added. This is useful to simply test the effects of the cadence on the derived velocity and acceleration profiles and their associated errors. Figure 3 shows a sample output of the test. Figures 3(a) and (b) show the model CME acceleration profile sampled at cadences of 3 and 10 mins respectively, relative to the initial point at 0 mins (blue) held fixed while the varying cadence changes the locations of the other sample points along the profile. Note that the errorbars of the two points at both the start and end of the interval are larger than the rest to account for not having enough points to interpolate across them (the endpoints of velocity having already undergone the same treatment). As the cadence is reduced, i.e., the cadence time is increased, the errorbars become smaller due to the inverse dependence of the Lagrangian error treatment on the time between points (Δt^{-2}). However, reducing the cadence reduces the resolution with which it is able to detect the acceleration peak, and so the peak is smoothed out until the interval is eventually approximated as being one of constant zero acceleration, as demonstrated in Figure 3(d) (where the non-smooth transition and errorbar sizes are as a result of stepping down in sample size such that the fixed point at 9 mins eventually becomes the start-point of the interval). Figure 3(c) shows the trend of derived acceleration on the fixed point at

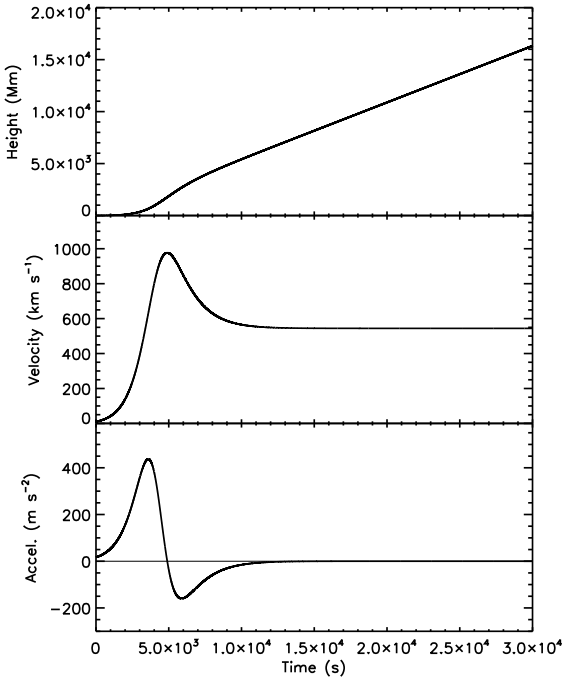

Fig. 2.— .

0 mins for increasing cadence time, corresponding directly to the start-point (blue) of the top two plots (a) and (b). In this case, as the cadence time is increased the derived acceleration value at the fixed 0 mins point approaches the true acceleration peak as the points average across the general peaked trend, before it is smoothed out and the interval is again approximated as having constant zero acceleration. Figures 3(c) and (d) clearly show the effect of the Δt^{-2} dependence of the errorbars derived through the 3-point Lagrangian interpolation, wherein the errors would become infinitely large for infinitely high cadence, and imply erroneously high precision for very low cadence sampling of the data. The importance of where along the profile the sample points are taken is also highlighted here.

It is also noted that the trend of the acceleration profile at high-cadence samplings is also revealed by the errorbars' span across the interval, as is shown in Figure 3(a) for example. This fundamentally implies that the errors do not truly reflect a 1 σ uncertainty on the data in this case, but recall here that no noise has been added to the dataset. The addition of noise, even to only a small degree, creates large problems for derivatives.

3.2. Bootstrapping/Spline Fits?

3.3. Inversion Techniques?

4. CORIMP Case Studies

5. Conclusions

REFERENCES

Gallagher, P. T., Lawrence, G. R., & Dennis, B. R. 2003, ApJ, 588, L53

Wen, Y., Maia, D. J. F., & Wang, J. 2007, ApJ, 657, 1117

This 2-column preprint was prepared with the AAS LaTeX macros v5.2.

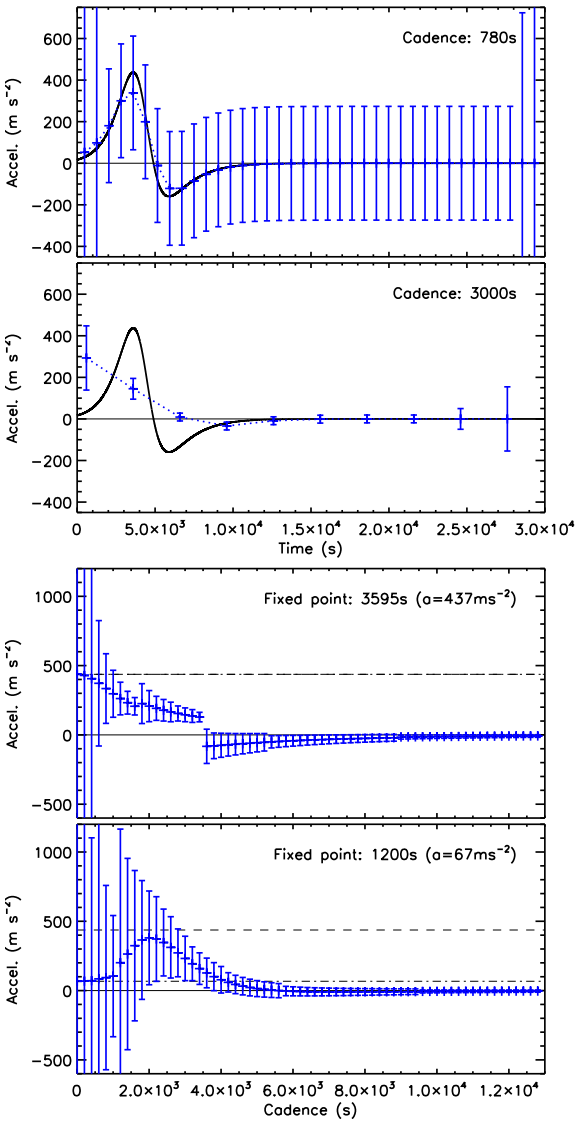

Fig. 3.— A demonstration of the effects of cadence on the error propagation according to the 3-point Lagrangian interpolation. A theoretical model for a CME with non-constant acceleration peaking at 676 m s^{-2} is tested for varying cadences of 1 to 47 mins. Plots (a) and (b) show the cases when the cadence is 3 mins and 10 mins respectively, relative to a fixed point at the 0 mins frame (start-point). Plots (c) and (d) show the derived acceleration values and associated errorbars as a function of cadence, relative to fixed points at 0 mins and 9 mins (peak acceleration point). The dotted line represents the peak acceleration value, and the dashed line represents the true acceleration expected in each case (which is the peak acceleration anyway for the case of the fixed point at 9 mins).